ELSEVIER

Journal of Organometallic Chemistry 506 (1996) 241–251

Journal of Organometallic Chemistry

Titanocene-bis(trimethylsilyl)acetylene complexes: effects of methyl substituents at the cyclopentadienyl ligands on the structure of thermolytic products

Vojtech Varga [a], Karel Mach [a,*], Miroslav Polášek [a], Petr Sedmera [b], Jörg Hiller [c], Ulf Thewalt [c], Sergei I. Troyanov [d]

[a] *J. Heyrovský Institute of Physical Chemistry, Academy of Sciences of the Czech Republic, Dolejškova 3, 182 23 Prague 8, Czech Republic*
[b] *Institute of Microbiology, Academy of Sciences of the Czech Republic, Prague 4, Czech Republic*
[c] *Sektion für Röntgen- und Elektronenbeugung, Universität Ulm, 89069 Ulm, Germany*
[d] *Department of Chemistry, Moscow State University, 119899 Moscow, Russia*

Received 30 March 1995

Abstract

The $(C_5H_{5-n}Me_n)_2Ti[\eta^2\text{-}C_2(SiMe_3)_2]$ ($n = 0$–5) (**1A–1F**) complexes were prepared by the reduction of corresponding titanocene dichlorides with magnesium in THF in the presence of bis(trimethylsilyl)acetylene (BTMSA). All of them were characterized by spectroscopic methods and $(C_5HMe_4)_2Ti[\eta^2\text{-}C_2(SiMe_3)_2]$ (**1E**) by the X-ray crystal analysis. The complexes decompose at temperatures in the range 100–200°C. Those with $n = 0$–3 yield (μ-η^5:η^5-fulvalene)(di-μ-hydrido)bis(η^5-cyclopentadienyltitanium) (**2A**) and its methylated analogues (**2B–2D**) whereas BTMSA is released. The crystal structure of **2D** showed that the hexamethylfulvalene ligand contains non-methylated carbon atoms in inner alternate positions. Complex **1E** afforded a mixture of products. Among them only volatile isomers (η^3:η^4-1,2-dimethyl-4,5-dimethylenecyclopentenyl)(η^5-tetramethylcyclopentadienyl)titanium (**2Ea**) and (η^3:η^4-1,3-dimethyl-4,5-dimethylenecyclopentenyl)(η^5-tetramethylcyclopentadienyl)titanium (2Eb) have been so far isolated as minor products. The C_5Me_5 complex **1F** yields quantitatively (η^3:η^4-1,2,3-trimethyl-4,5-dimethylenecyclopentenyl)(pentamethylcyclopentadienyl)titanium (**2F**) and BTMSA is hydrogenated to a mixture of *cis*- and *trans*-bis(trimethylsilyl)ethene.

Keywords: Titanium; Titanocene; Thermolysis; (Trimethylsilyl)acetylene complexes

1. Introduction

Titanocene moieties Cp'_2Ti^{II} for $Cp' = C_5H_5$ and C_5Me_5 are known to be stabilized by coordination of ligands like CO, phosphines or acetylenes which are able to accommodate Ti^{II} d^2 electrons in low-energy LUMO orbitals [1,2]. The first titanocene–acetylene complexes were obtained by partial replacement of carbon monoxide [3] or a trialkylphosphine [4] by diphenylacetylene or bis(pentafluorophenyl)acetylene [5]. The complexes of dialkylacetylenes and diphenylacetylene were prepared either by the displacement of ethylene from the $(C_5Me_5)_2Ti(\eta^2\text{-}C_2H_4)$ complex [6] or by the acetylene coordination to the $(C_5H_5)_2Ti$ species generated in the $(C_5H_5)_2TiCl_2/Mg/THF$ systems [7]. The dialkylacetylene and diphenylacetylene complexes are highly reactive towards acetylenes to give titanacyclopentadiene derivatives and low yields of catalytically formed hexasubstituted benzenes. Thus, only the titanocene–diphenylacetylene complexes were isolated and characterized by spectroscopic and chemical means [6,7]. In contrast, the bis(trimethylsilyl)-acetylene (BTMSA) complexes $(C_5H_5)_2Ti[\eta^2\text{-}C_2(SiMe_3)_2]$ [8] and $(C_5Me_5)_2Ti[\eta^2\text{-}C_2(SiMe_3)_2]$ [9] were obtained in high yields by the reduction of titanocene dichlorides with one equivalent of magnesium in the presence of excess BTMSA. The X-ray crystal data were published for the latter complex and both the complexes were characterized by ^1H and ^{13}C NMR and IR spectra [10]. These complexes do not form titanacyclopentadiene complexes and do not enter addition reac-

* Corresponding author.

SSDI 0022-328X(95)05758-7

tions. Instead, BTMSA is displaced by coordinatively stronger reagents, including diphenylacetylene [8]. The phenyl(trimethylsilyl)acetylene complexes $(C_5Me_5)_2Ti[C_2(C_6H_5)(SiMe_3)]$ and $(C_5H_5)_2Ti[C_2(C_6H_5)(SiMe_3)]$ were prepared analogously and their X-ray crystal structures revealed distinct structure differences in the acetylene ligands created by steric hindrance due to the C_5Me_5 ligand [11].

The BTMSA complexes should be suitable reagents for the generation of titanocene species because (a) they are thermally stable at ambient temperature although BTMSA is, as follows from the value of $\Delta\nu(C{\equiv}C)$ [12], less strongly coordinated than diphenylacetylene, and (b) the coordinated BTMSA does not undergo addition reactions with free BTMSA. The thermal treatment of the $(C_5H_{5-n}Me_n)_2Ti[\eta^2\text{-}C_2(SiMe_3)_2]$ ($n = 0$–5) complexes (**1A–1F**) thus should allow us to study rearrangement pathways of thermally much less stable titanocene $(C_5H_{5-n}Me_n)_2Ti^{II}$ ($n = 0$–5) species as depending on the number of electron donating Me substituents at the cylopentadienyl rings.

Here we report the preparation of the whole series of the $(C_5H_{5-n}Me_n)_2Ti[\eta^2\text{-}C_2(SiMe_3)_2]$ ($n = 0$–5) (**1A–1F**) complexes, their spectroscopic characteristics, products of their thermal decomposition, and crystal structures of **1E** and the product of thermolysis of **1D**.

2. Experimental details

All manipulations with reagents, synthesis, and most of spectroscopic measurements were carried out under vacuum using all-sealed glass devices equipped with breakable seals. The adjustment of single crystals into capillaries for X-ray analysis, preparation of KBr pellets and filling of infrared KBr cuvettes were performed in an atmosphere of nitrogen or argon.

2.1. Chemicals

The solvents THF, hexane, toluene, and benzene-d_6 were purified by conventional methods, dried by refluxing over $LiAlH_4$ and stored as solutions of dimeric titanocene $(C_{10}H_8)[(C_5H_5)Ti(\mu\text{-}H)]_2$ [13]. Bis(trimethylsilyl)acetylene (BTMSA) (Fluka) was degassed, stored as a solution of dimeric titanocene for 4 h and distilled in vacuum into ampoules. Magnesium turnings (Fluka, purum for Grignard reactions) were weighed and evacuated. Titanocene dichlorides $(C_5H_{5-n}Me_n)_2TiCl_2$ ($n = 0$–5) were prepared according to literature procedures: $(C_5H_5)_2TiCl_2$ and $(C_5H_4Me)_2TiCl_2$ [14], $(C_5H_3Me_2)_2TiCl_2$ (1,3-dimethyl) [15], and $(C_5H_2Me_3)_2TiCl_2$ (1,2,3-trimethyl), $(C_5HMe_4)_2TiCl_2$ and $C_5Me_5)_2TiCl_2$ [16] and were finally purified by crystallization from toluene.

2.2. Methods

^1H and ^{13}C NMR spectra were measured on a Varian VXR-400 spectrometer (400 and 100 MHz, respectively) in C_6D_6 at 25°C. Chemical shifts (given in the δ scale) were referenced to the solvent signal (δ_H 7.15 ppm, δ_C 128.0 ppm). Assignment of spectra of the $C_5H_{5-n}Me_n$ ligands was carried out using a delayed COSY experiment. ^{29}Si NMR spectra were taken on a Varian XL spectrometer using a routine version of the INEPT pulse sequence [17]. UV-Vis spectra were measured in the range 270–2000 nm on a Varian Cary 17D spectrometer using all-sealed quartz cuvettes (Hellma). Mass spectra were measured on a JEOL D-100 spectrometer at 75 eV (only important mass peaks and peaks of intensity $\geqslant 5\%$ are reported). Samples in capillaries were opened and inserted into the direct inlet under argon. Infrared spectra were obtained on a UR-75 (Ziess, Jena, Germany) or on a Mattson Galaxy 2020 spectrometer. Hexane solutions were filled into KBr cuvettes under argon; regions 2800–3000 cm^{-1} and 1400–1500 cm^{-1} were not registered. KBr pellets from estimated amounts of solid samples were prepared in a glovebox under purified nitrogen and were measured in a cuvette under the nitrogen atmosphere. GC analysis of volatile products of thermolysis of **1A–1F** were performed on a CHROM 5 gas chromatograph (Laboratory Instruments, Prague, Czech Republic) using 10% SE-30 on a Chromaton N-AW-DMCS column. Analogous GC-MS analyses were carried out on a Hewlett Packard gas chromatograph (5890 series II) equipped with a mass spectrometric detector (5971 A) and a capillary column SPB-1 (Supelco).

2.3. Preparation of $(C_5H_{5-n}Me_n)_2Ti[\eta^2\text{-}C_2(SiMe_3)_2]$ ($n = 0$–5) complexes 1A–1F

$(C_5H_{5-n}Me_n)_2TiCl_2$ (2 mmoles) and Mg (0.0486 g, 2 mmoles) were charged into an ampoule equipped with a teflon-coated magnetic stirrer. The ampoule was evacuated and BTMSA (0.5 ml, 2.2 mmol) and THF (30 ml) were distilled in on a vacuum line. The mixture was frozen by liquid nitrogen, sealed off and stirred at room temperature for 2 days. A clear yellow solution was obtained after all the magnesium had dissolved. THF was evaporated on a vacuum line with final heating to 60°C and a yellow residue was extracted by hexane. Yellow crystalline materials were obtained by cooling of concentrated solutions for $n = 2$–5 whereas compounds for $n = 0$ and 1 formed amorphous solids. All the compounds were obtained in nearly quantitative yields. Alternatively, magnesium metal was used in an excess (typically Mg:Ti = 50) to shorten the reaction time to several hours. This was advantageous for obtaining **1D–1F** which appeared to be unreactive towards magnesium. Somewhat irreproducible induction period

was eliminated by using an activated metal, isolated from a preceding experiment. When using excess magnesium for obtaining **1A–1C**, the reaction had to be quickly terminated by pouring off the reaction solution from magnesium when the solution turned yellow. This is to be done to avoid the reaction of **1A–1C** with magnesium yielding binuclear Ti–Mg complexes $[(C_5H_{5-n}Me_n)Ti][\mu:\eta^2:\eta^2\text{-}C_2(SiMe_3)_2]_2[(C_5H_{5-n}Me_n)Mg]$ and/or trinuclear Ti–Mg–Mg complexes $[(C_5H_{5-n}Me_n)Ti][\mu\text{-}\eta^2:\eta^2\text{-}C_2(SiMe_3)_2]_2[Mg(\mu\text{-}Cl)_2]\text{-}[(C_5H_{5-n}Me_n)Mg(THF)]$ [15,18]. Since the termination of the reaction is not well defined and the purification of **1A–1C** by fractional crystallization is time consuming we recommend using one equivalent of Mg with respect to $(C_5H_{5-n}Me_n)_2TiCl_2$.

$(C_5H_5)_2Ti[\eta^2\text{-}C_2(SiMe_3)_2]$ (**1A**). ^{1}H NMR (C_6D_6): δ −0.333 (s, 18H, 2 × $SiMe_3$); 6.410 (s, 10H). ^{13}C NMR (C_6D_6): δ 0.59 (q, 6C, 2 × $SiMe_3$); 117.82 (d, 10C); 244.77 (s, 2C, C≡C). ^{29}Si NMR: δ −14.41. UV-Vis (λ_{max}, hexane): 1060 (br) < < 360 (sh) < 272 (sh) nm. IR (KBr, cm^{-1}): 1720w, sh, 1688s, 1643m, sh, 1600w, sh, 1480w, 1437m, 1398w, 1240s, 1122w, 1067vw, 1013s, 850vs, 832vs, 793vs, 746s, 685m, 643m, 614m, 473w, 406m. MS (m/e, (%)): 348(M^+; 2.2), 178(100), 170(5.5), 155(45).

$(C_5H_4Me)_2Ti[\eta^2\text{-}C_2(SiMe_3)_2]$ (**1B**). ^{1}H NMR (C_6D_6): δ −0.270 (s, 18H, 2 × $SiMe_3$); 2.095 (s, 6H, 2 × Me); 5.395 (dd, 4H, 2 × H-3, 4, J = 2.7 Hz); 6.442 (dd, 4H, 2 × H-2, 5, J = 2.7 Hz). ^{13}C NMR (C_6D_6): δ 1.18 (q, 6C); 16.98 (q, 2C); 114.08 (d, 4C, 2 × C-2, 5); 115.90 (d, 4C, 2 × C-3, 4); 130.92 (s, 2C, 2 × C-1); 245.28 (s, 2C, C≡C). ^{29}Si NMR: δ −15.41. UV-Vis (λ_{max}, hexane): 990 (br) < < 350 (sh) < 272 (sh) nm. IR (KBr, cm^{-1}): 1720w, sh, 1674m, 1638m, 1604w, sh, 1242s, 1078w, 1044m, 1024m, 936w, 858vs, 825vs, 790vs, 750s, 686m, 644m, 614m, 468m, 408m. MS (m/e, (%)): 376(M^+; 1.4), 206(100), 170(7), 155(74).

$(C_5H_3Me_2)_2Ti[\eta^2\text{-}C_2(SiMe_3)_2]$ (**1C**). ^{1}H NMR (C_6D_6): δ −0.228 (s, 18H, 2 × $SiMe_3$); 1.606 (s, 12H, 4 × Me); 5.735 (d, 4H, 2 × H-4, 5, J = 2.4 Hz); 6.530 (t, 2H 2 × H-2, J = 2.4 Hz). ^{13}C NMR (C_6D_6): δ 1.54 (q, 6C); 15.90 (q, 4C, Me-1, 3); 115.54 (d, 4C, 2 × C-4, 5); 116.13 (d, 2C, 2 × C-2); 128.17 (s, 4C, 2 × C-1, 3); 245.54 (s, 2C, C≡C). ^{29}Si NMR: δ −16.06. UV-Vis (λ_{max}, hexane): 985(br) < < 352 (sh) < 270(sh) nm. IR (KBr, cm^{-1}): 1720w, 1670m, 1630s, 1608w, sh, 1510m, 1460m, 1435m, 1375m, 1240s, 1136w, 1050w, 1028m, 945w, 858vs, 822vs, 796vs, sh, 746s, 682m, 645m, 613m, 465m, 418m. MS (m/e, (%)): 404(M^+; 1.0), 234(100), 170(5.0), 155(45.0).

$(C_5H_2Me_3)_2Ti[\eta^2\text{-}C_2(SiMe_3)_2]$ (**1D**). ^{1}H NMR: δ −0.118 (s, 18H, 2x$SiMe_3$); 1.480 (s, 12H, 2 × 1, 3-Me); 1.925 (s, 6H, 2 × 2-Me); 5.816 (s, 4H, 2 × 4, 5-H). ^{13}C NMR: δ 2.31 (q, 6C); 12.61 (q, 2C, 2 × 2-Me); 14.17 (q, 4C, 2 × 1, 3-Me); 113.64 (d, 4C, 2 × C-4, 5); 124.19 (s, 2C, 2 × C-2); 124.70 (s, 4C, 2 × C-1, 3); 246.35 (s, 2C, C≡C). ^{29}Si NMR: δ −16.36. UV-Vis (λ_{max}, hexane): 915(br) < < 350(sh) < 260(sh) nm. IR (KBr, cm^{-1}): 1663m, 1618s, 1600m, sh, 1490m, 1445m, 1377w, 1242s, 1074w, 1023w, 858vs, 831s, 782s, 748s, 684m, 650m, 617w, 448m, 424m. MS (m/e, (%)): 432(M^+; 0.5), 262(48), 170(5.5), 155(100).

$(C_5HMe_4)_2Ti[\eta^2\text{-}C_2(SiMe_3)_2]$ (**1E**). ^{1}H NMR: δ −0.049 (s, 18H, 2 × $SiMe_3$); 1.301 (s, 12H, 2 × 1, 4-Me); 2.116 (s, 12H, 2 × 2,3-Me); 5.093 (s, 2H, 2 × 5-H). ^{13}C NMR: δ 3.46 (q, 6C); 13.50 (q, 4C, 1, 4-Me); 13.57 (q, 4C, 2x2, 3-Me); 113.00 (d, 2C, 2 × C-5); 121.53 (s, 4C, 2 × C-1, 4); 125.02 (s, 4C, 2xC-2, 3); 248.35 (s, 2C, C≡C). ^{29}Si NMR: δ −17.18. UV-Vis (λ_{max}, hexane): 920(br) < < 375(sh) < 255(sh) nm. IR (KBr, cm^{-1}): 1658w, 1602m, sh, 1568s, 1484w, 1441m, 1378w, 1362w, 1240s, 1020w, 850vs, 835vs, 750s, 679m, 658m, 617m, 450m, 419m. MS (m/e, (%)): 290(43), 170(7), 155(100).

$(C_5Me_5)_2Ti[\eta^2\text{-}C_2(SiMe_3)_2]$ (**1F**). ^{1}H NMR: δ 0.016 (s, 18H, 2 × $SiMe_3$); 1.718 (s, 30H, 10Me); ^{13}C NMR: δ 4.23 (q, 6C); 12.72 (q, 10C); 121.97 (s, 10C); 248.51 (s, 2C, C≡C). ^{29}Si NMR: δ −17.29. UV-Vis (λ_{max}, hexane): 916(br) < < 395(sh) < 263(sh) nm. IR (KBr, cm^{-1}): 1638w, 1595m, 1562m, 1487w, 1445m, 1377w, 1242s, 1022w, 850vs, 837vs, 752s, 677m, 656m, 618m, 449m, 424m. MS (m/e, (%)): 318(100), 303(6.7), 170(2.0), 155(20).

Infrared spectra of **1A–1F** (bands of low information value in the region 2890–3100 cm^{-1} are not listed) in hexane solutions agreed with the spectra of samples in KBr pellets within the maximum difference in the band position ±4 cm^{-1}. Different intensities of absorption bands in these two media were most remarkable for the bands belonging to ν(C≡C) vibration of coordinated BTMSA.

2.4. Thermal decomposition of 1A–1F

Solid complexes (2 mmoles) as prepared above were dissolved in 10 ml of dry degassed m-xylene. The solutions were heated in sealed ampoules to a temperature in the range 100–200°C with accuracy ±0.5°C. After cooling to ambient temperature the presence of eventually evolved hydrogen was controlled after attachment to a vacuum line, always with a negative result. All volatiles were distilled in a closed system at maximum 60°C into an ampoule cooled to 77 K overnight. The volatiles were identified by GC and/or GC-MS. Contents of the products, mainly BTMSA or a mixture of *cis*- and *trans*-bis(trimethylsilyl)ethene were calibrated with respect to a standard concentration of BTMSA in m-xylene (0.2 mol l^{-1}). A solid remainder was extracted with hexane (20 ml). The concentrated hexane solutions yielded crystalline materials for **1A–1D** and **1F**. Evaporation of solvents from products of **1E** gave a brown residue which did not yield any individual

product by crystallization methods, however, a blue product was obtained by sublimation in vacuo at 110°C. It afforded a crystalline material by cooling of concentrated hexane solution. All the crystalline products (**2A–2F**) were used for the preparation of solutions in hexane, toluene or C_6D_6 for spectroscopic characterization and **2D** for the X-ray crystal structure analysis.

From **1A**: (μ-η^5:η^5-$C_{10}H_8$)[(η^5-C_5H_5)Ti(μ-H)]$_2$ (**2A**). Bright green finely crystalline solid, yield 85%. UV-Vis (λ_{max}, hexane): 432 < 780(sh) < 828 nm. IR (benzene): ν(Ti–H) 1227 cm^{-1}. MS (direct inlet, m/e(%)): 356(M^+, 23), 355(27), 354(65), 353(44), 352(100), 351(39), 350(55), 349(23), 348(28), 347(9), 346(7) (cf. [19]).

From **1B**: (μ-η^5:η^5-$C_{10}H_6Me_2$)[(η^5-C_5H_4Me)-Ti(μ-H)]$_2$ (**2B**). Green crystalline solid, yield 80%. UV-Vis (λ_{max}, hexane): 432 < 770(sh) < 828 nm. IR (hexane): ν(Ti–H) 1213 cm^{-1}. MS (direct inlet, m/e(%)): 412 (M^+, 44), 411(40), 410(81), 409(50), 408(90), 407(52), 406(100), 405(51), 404(78), 403(35), 402(41), 401(18), 400(18), 399(9), 398(9), 397(6), 396(10), 395(8), 394(13), 393(13), 392(15), 391(13), 390(11), 389(7), 388(7), 387(5).

From **1C**: (μ-η^5:η^5-$C_{10}H_4Me_4$)[(η^5-$C_5H_3Me_2$)-Ti(μ-H)]$_2$ (**2C**). Green crystalline solid, yield 63%. UV-Vis (λ_{max}, hexane): 310, 434 < 770(sh) < 840 nm. IR (hexane): ν(Ti–H) 1206, 1180(sh) cm^{-1}; (KBr): 1200(sh), 1186 cm^{-1}. MS (direct inlet, m/e(%)): 468(M^+, 59), 467(52), 466(96), 465(57), 464(97), 463(59), 462(100), 461(60), 460(95), 459(39), 458(59), 457(30), 456(43), 455(22), 454(20), 453(11), 452(10), 451(6), 450(5), 447(5), 446(7), 445(11), 444(9), 443(13), 442(9), 441(9), 440(5), 439(5).

From **1D**: (μ-η^5:η^5-$C_{10}H_2Me_6$)[(η^5-$C_5H_2Me_3$)-Ti(μ-H)]$_2$ (**2D**). Yellow-green crystals, yield 56%. UV-Vis (λ_{max}, hexane): 434 < 780(sh) < 862 nm. IR (hexane): ν(Ti–H) 1166, 1134(sh) cm^{-1}; (KBr): 1167(sh), 1116 cm^{-1}. MS (direct inlet, m/e(%)): 524(M^+, 17), 523(22), 522(48), 521(34), 520(61), 519(42), 518(70), 517(60), 516(100), 515(42), 514(52), 513(21), 512(28), 511(12), 510(14), 509(8), 508(8), 507(6), 506(6), 505(5), 504(4), 503(5), 502(6), 501(11), 500(10), 499(16), 498(11), 497(13), 496(7), 495(6), 494(4).

From **1E**: blue crystalline solid sublimed at 110°C in vacuo, yield 0.05 g (8%). ^{1}H and ^{13}C NMR (C_6D_6, 23°C): the spectra were assigned to a mixture of symmetric (η^3:η^4-1,3-dimethyl-4,5-dimethylenecyclopentenyl)(η^5-tetramethylcyclopentadienyl)titanium (**2Ea**) and asymmetric (η^3:η^4-1,2-dimethyl-4,5-dimethylenecyclopentenyl)(η^5-tetramethylcyclopentadienyl)-titanium (**2Eb**) in the ratio ca. 8:1. The NMR spectra of the two components were identical with those found earlier in a similar mixture [20].

From **1F**: (η^3:η^4-1,2,3-trimethyl-4,5-dimethylenecyclopentenyl)(pentamethylcyclopentadienyl)titanium (**2F**). Blue crystalline solid was obtained by evaporation of hexane. It was sublimed in vacuum at 130°C to give 0.58 g (92%) of blue finely crystalline solid. ^{1}H and ^{13}C NMR in C_6D_6, MS (direct inlet, 50°C) and UV-Vis spectra in hexane were in full agreement with the previously reported ones [20,21].

2.5. X-ray crystal structure analysis of 1E

A crystal fragment of dimensions 0.2 × 0.3 × 0.3 mm was fixed in a capillary under argon. Data were collected on an Enraf-Nonius CAD-4 diffractometer using graphite-monochromated Mo–K_α radiation at room temperature. The structure was solved by direct methods and Fourier syntheses. All non-hydrogen atoms were refined anisotropically. All hydrogen atoms were found in the difference Fourier synthesis and then refined isotropically. Crystallographic calculations were carried out using SDP programs. Crystallographic data are summarized in Table 1. Atom coordinates are listed in Table 2. Selected bond distances and bond angles are given in Table 3.

2.6. X-ray crystal structure analysis of μ-(η^5:η^5-2,3,4,3′,4′,5′-hexamethylfulvalene)-di-(μ-hydrido)-bis-[(η^5-1,2,3-trimethylcyclopentadienyl)titanium(III)], 2D

A crystal fragment was selected and mounted into a Lindemann glass capillary under purified nitrogen in a glovebox (Braun). The capillary was closed with sealing

Table 1
Crystallographic data and experimental details for **1E** and **2D**

	1E	2D
(a) Crystal data		
Chem. formula	$C_{26}H_{44}Si_2Ti$	$C_{32}H_{44}Ti_2$
Mol.wt (g mol^{-1})	460.69	524.46
Crystal system	monoclinic	monoclinic
Space group	$C2/c$, No. 15	$P2_1/c$, No. 14
a (Å)	15.086(2)	14.720(6)
b (Å)	10.571(2)	17.016(3)
c (Å)	17.780(4)	11.522(4)
β (°)	104.94(2)	106.84(2)
Z	4	4
Volume (Å^3)	2739.5	2762(2)
$D_{calc.}$ (g cm^{-3})	1.12	1.26
μ(Mo K α) (cm^{-1})	4.04	5.44
Approx. cryst. dimensions [mm]	0.2×0.3×0.3	0.2×0.3×0.4
(b) Data collection and refinement		
$2\theta_{max}$ (°)	< 50	< 48
Unique observed reflections		
total	2513	4779
$I \geq 3\sigma(I)$	1651	$I \geq \sigma(I)$ 2427
No. of variables	220	307
R	0.037	0.092
R_w	0.042	0.096

Table 2
Atomic coordinates and equivalent isotropic temperature factors for non-hydrogen atoms in **1E** [a]

Atom	x	y	z	U_{eq} (Å^2)
Ti(1)	0.0000	0.0645(1)	0.2500	0.030(1)
Si(1)	−0.0135(1)	0.3758(1)	0.1361(1)	0.043(1)
C(1)	−0.0049(2)	0.2539(3)	0.2125(2)	0.031(1)
C(2)	−0.1285(3)	0.4552(4)	0.1117(3)	0.068(1)
C(3)	0.0732(3)	0.5047(4)	0.1690(3)	0.075(1)
C(4)	0.0046(4)	0.3053(5)	0.0446(2)	0.086(1)
C(5)	0.1184(2)	−0.0717(4)	0.3188(2)	0.043(1)
C(6)	0.1590(2)	0.0491(4)	0.3239(2)	0.046(1)
C(7)	0.1617(2)	0.0849(3)	0.2480(2)	0.040(1)
C(8)	0.1217(2)	−0.0117(4)	0.1964(2)	0.049(1)
C(9)	0.0968(2)	−0.1080(3)	0.2406(2)	0.057(1)
C(51)	0.1124(3)	−0.1542(5)	0.3877(3)	0.075(1)
C(61)	0.2038(3)	0.1197(5)	0.3974(3)	0.083(1)
C(71)	0.2068(3)	0.2021(4)	0.2280(3)	0.071(1)
C(81)	0.1119(3)	−0.0144(5)	0.1099(2)	0.092(1)

[a] Atoms Si(1'), C(1'), etc. are related to atoms Si(1), C(1), respectively, etc., by the symmetry operation $-x, y, \frac{1}{2} - z$.

Table 3
Selected bond distances [Å] and bond angles [°] for **1E** and **1F** [a]

	1E	**1F**	
Distances			
Ti(1)–C(1)	2.106(3)	2.122(3)	2.126(3)
Ti(1)–CE(Cp ring)	2.092(4)	[b]	
Ti(1)–C(Cp ring) (av.)	2.41(3)	2.435	2.427
C–C(Cp ring) (av.)	1.403(7)	1.414	1.414
C(Cp ring)–C(Me) (av.)	1.509(9)	1.503	1.500
C(1)–C(1')	1.303(5)	1.309(4)	
Si(1)–C(1)	1.853(3)	1.862(3)	1.856(3)
Si(1)–C(2)	1.875(5)	1.869(4)	1.871(4)
Si(1)–C(3)	1.875(5)	1.870(4)	1.870(4)
Si(1)–C(4)	1.872(5)	1.876(5)	1.878(5)
Angles			
C(1)–Ti(1)–C(1')	36.0(1)	[b]	
Ti(1)–C(1)–C(1')	72.0(2)	[b]	
CE–Ti(1)–CE'	134.9(1)	[b]	
Si(1)–C(1)–C(1')	135.9(3)	134.8(3)	136.8(3)
ϕ [c]	50.0	41.1	

[a] Taken from ref. [10]; the two values stem from the absence of symmetry element.
[b] Data not given.
[c] Dihedral angle between least squares planes of cyclopentadienyl rings.

wax. The unit cell parameters and intensities of 4779 reflections were measured on a Philips PW 1100 four circle diffractometer equipped with a STOE electronic control system at room temperature by the $\theta/2\theta$ method, using graphite monochromated MoK_α radiation ($\lambda = 0.71069$ Å). The structure was solved by iterative symbolic addition and refined with anisotropic temperature factors for the non-hydrogen atoms. Due to insufficient quality of the measured data the bridging hydrogen atoms could not be located in the difference electron density map. These as well as the other hydrogen atoms were not included in the refinement. All calculations were performed by use of the PC-ULM-package incorporating the SHELX-76 program [22]. Further details of data collection and refinement are summarized in Table 1. Atomic coordinates for the non-hydrogen atoms are listed in Table 4. Selected bond lengths and bond angles are given in Table 5.

3. Results and discussion

All the $(C_5H_{5-n}Me_n)_2Ti[\eta^2\text{-}C_2(SiMe_3)_2]$ ($n = 0$–5) complexes (**1A–1F**) were prepared in high yields by the general method consisting in the reduction of the $(C_5H_{5-n}Me_n)_2TiCl_2$ complexes by one molar equivalent of magnesium in THF in the presence of at least one molar equivalent of BTMSA (eqn. (1)).

$$(C_5H_{5-n}Me_n)_2TiCl_2 + Mg + C_2(SiMe_3)_2 \xrightarrow{THF} (C_5H_{5-n}Me_n)_2Ti[\eta^2\text{-}C_2(SiMe_3)_2] + MgCl_2 \quad (1)$$

This method was previously used for obtaining **1A** and **1F** [8–10]. An irreproducible induction period, which occurs when commercial magnesium turnings are used, is removed and the formation of **1A–1F** is speeded up by using an excess of activated magnesium which has been obtained from a preceding experiment and has not been exposed to air. This is advantageous for the preparation of **1D–1F** as they are inert towards magnesium metal. However, for **1A–1C** the reaction solution has to be quickly separated from magnesium when the colour of the solution turns yellow. This is because compounds **1A–1C** react further with magnesium to give binuclear Ti–Mg and trinuclear Ti–Mg–Mg complexes containing perpendicularly bridging BTMSA ligands, $[Cp'Ti][\mu:\eta^2:\eta^2\text{-}C_2(SiMe_3)_2]_2[Cp'Mg]$ and $[Cp'Ti][\mu\text{-}\eta^2:\eta^2\text{-}C_2(SiMe_3)_2]_2[Mg(\mu\text{-}Cl)_2][Cp'Mg(THF)]$ [15,18]. Since the quantitative separation of

Table 4
Atomic coordinates and equivalent isotropic temperature factors for non-hydrogen atoms in **2D**

Atom	x	y	z	U_{eq} (Å^2)
Ti(1)	0.2967(1)	−0.0840(1)	0.2067(2)	0.035(1)
Ti(2)	0.2037(1)	0.0606(1)	0.2893(2)	0.040(1)
C(1)	0.2387(6)	−0.1165(5)	0.3648(8)	0.035(5)
C(2)	0.3383(7)	−0.1397(5)	0.4050(9)	0.043(5)
C(21)	0.4155(8)	−0.1090(7)	0.510(1)	0.061(6)
C(3)	0.3453(8)	−0.2037(6)	0.331(1)	0.052(6)
C(31)	0.4354(9)	−0.2543(7)	0.350(1)	0.072(7)
C(4)	0.2566(8)	−0.2199(6)	0.248(1)	0.048(6)
C(41)	0.2318(9)	−0.2856(6)	0.152(1)	0.072(7)
C(5	0.1913(7)	−0.1670(5)	0.2633(9)	0.043(5)
C(6)	0.1975(7)	−0.0473(5)	0.4059(8)	0.037(5)
C(7)	0.2465(6)	0.0124(5)	0.4885(8)	0.039(5)
C(8)	0.1815(7)	0.0716(5)	0.4933(8)	0.041(5)
C(81)	0.2037(9)	0.1388(7)	0.586(1)	0.067(7)
C(9)	0.0933(7)	0.0529(5)	0.4161(8)	0.039(5)
C(91)	0.0006(7)	0.0948(7)	0.406(1)	0.066(6)
C(10)	0.1013(7)	−0.0201(6)	0.3593(8)	0.040(5)
C(101)	0.0161(8)	−0.0626(7)	0.278(1)	0.067(7)
C(11)	0.4378(7)	0.0854(6)	0.1447(8)	0.042(5)
C(111)	0.5361(8)	−0.0825(9)	0.242(1)	0.084(7)
C(12)	0.3933(9)	−0.0181(6)	0.083(1)	0.061(6)
C(121)	0.4366(9)	0.0616(6)	0.095(1)	0.075(7)
C(13)	0.3045(7)	−0.0432(7)	0.001(1)	0.051(6)
C(131)	0.235(1)	0.0033(8)	−0.096(1)	0.086(8)
C(14)	0.2993(8)	−0.1260(7)	0.013(1)	0.055(6)
C(15)	0.3826(7)	−0.1526(6)	0.0988(9)	0.045(5)
C(16)	0.2564(9)	0.1928(8)	0.283(2)	0.091(8)
C(161)	0.329(1)	0.2353(9)	0.379(2)	0.17(1)
C(17)	0.1562(8)	0.1991(5)	0.264(1)	0.051(6)
C(171)	0.111(1)	0.2535(7)	0.331(1)	0.088(8)
C(18)	0.109(1)	0.1580(8)	0.154(1)	0.092(8)
C(181)	−0.003(1)	0.156(1)	0.097(2)	0.16(1)
C(19)	0.188(3)	0.130(1)	0.110(2)	0.18(1)
C(20)	0.269(2)	0.151(1)	0.188(2)	0.17(1)

unreacted magnesium from the solution is difficult to manage at the completion of the reaction leading to **1A–1C** and the separation of the formed binuclear Ti–Mg complexes is difficult, high purity compounds **1A–1C** are preferably obtained by using one equivalent of magnesium with respect to $(C_5H_{5-n}Me_n)_2TiCl_2$ (n = 0–2).

Compounds **1A–1F** form yellow solids, highly soluble in hexane. The crystalline samples were obtained by repeated crystallization from cooled hexane solutions. The ESR spectra were measured of the solutions made from crystalline fractions to control the content of paramagnetic impurities. Only the samples with negligible content of the impurities were used for final crystalliza-

Table 5
Selected bond distances (Å) and bond angles (°) for **2D**

Distances			
Ti(1)–CE(1)	2.063(10)	Ti(2)–CE(2)	2.064(10)
Ti(1)–CE(3)	2.104(11)	Ti(2)–CE(4)	2.060(18)
Ti(1)–C(1)	2.291(9)	Ti(2)–C(6)	2.293(10)
Ti(1)–C(2)	2.384(10)	Ti(2)–C(7)	2.346(10)
Ti(1)–C(3)	2.475(11)	Ti(2)–C(8)	2.475(10)
Ti(1)–C(4)	2.465(11)	Ti(2)–C(9)	2.484(10)
Ti(1)–C(5)	2.325(10)	Ti(2)–C(10)	2.347(10)
C–C(av) (CE(1) ring)	1.417(15)	C(1)–C(6)	1.465(13)
C–C(av) (CE(2) ring)	1.416(15)	Ti(1)...Ti(2)	3.096(2)
Angles			
CE(1)–Ti(1)–CE(3)	133.1(1)	CE(2)–Ti(2)–CE(4)	138.4(1)

tion to obtain crystals for the X-ray crystal analysis, KBr pellet preparation and for preparing solutions for UV-VIS-NIR, NMR and MS spectra. Compounds **1A–1F** do not show any ESR signal in the temperature range −196–+23°C and well-resolved ^{1}H and ^{13}C NMR spectra are compatible with the π-coordinated BTMSA ligand as found by the X-ray crystal structure analyses for **1F** [10] and **1E** (vide infra). Although the compounds behave like the derivatives of Ti(II), e.g. in their reaction with 2,2′-bipyridyl [23], their electronic absorption spectra show only one absorption band at 900–1000 nm (ϵ = 100–130 cm^2 $mmol^{-1}$) in the range 500–2500 nm which is not typical of the Ti(II) d^2 ion. This absorption band can be accounted for by the residence of both d^2 electrons in a low energy non-bonding orbital of the coordinated acetylene and arises from a CT $\pi^* \rightarrow$ d transition.

The infrared spectra of all **1A–1F** complexes show a cluster of bands in the region 1560–1720 cm^{-1} where valence vibrations of the coordinated BTMSA ligand occur (Table 6). The wavenumbers of the most intense bands of **1A** and **1F** agree with the literature data [10,12]. The bands of lower intensity were not reported but we observed them reproducibly for all compounds of the series in the samples which afforded the NMR spectra of a single compound and in the solid sample of **1E** from which a single crystal for the X-ray structure determination (vide infra) was selected. The reason for the occurrence of more bands has to be sought in the coupling of the C≡C valence vibration with vibrational modes of C–$SiMe_3$ groups and Ti–C_{ac} bonds.

The Me substituents at cyclopentadienyl rings unequivocally increase the strength of the Ti–acetylene bond. The evidence is obtained namely from large low-field shifts of δ (C≡C) resonance and a decrease in the average wavenumber of all the ν(C≡C) vibrations from 1662 cm^{-1} for **1A** to 1598 cm^{-1} for **1F** (Table 6). The latter values are unweighted with respect to their intensities and thus a great difference between the average wavenumbers for **1C** and **1D** arises from the absence of a weak absorption band at 1720 cm^{-1} in the **1D–1F** compounds. Intensities of these bands depend strongly on the sample medium (hexane versus KBr) and the evaluation of these effects is behind the scope of this work.

The NMR shifts of elements of the ≡$CSi(CH_3)_3$ group do not afford equal increments per one Me group but their trends are continuous (Table 6) and correspond to the expected shielding effects. The above mentioned NMR and IR shifts for the acetylenic group are so large that the acetylenic group in these complexes is considered to be a four electron donor or a constituent of a titanacyclopropene complex [12]. In fact, the low field shift δ(C≡C) in the [Cp′Ti][μ:η^2:η^2-$C_2(SiMe_3)_2$]$_2$-[Cp′Mg] complexes, where the acetylene ligands should be η^2-coordinated to both the Ti and Mg atoms, is by about 20 ppm larger than in **1A–1C** and the ν(C≡C) vibration is also shifted close to 1500 cm^{-1} [15]. The mass spectra of all compounds of the series show that the elimination of BTMSA ligand is far the most abundant process following the electron impact. The molecular ions were observed for only **1A–1D** and their intensity decreased from 2.2% for **1A** to 0.5% for **1D**. The main fragmentation ions were $[Cp'_2Ti]^+$ for **1A–1C** and **1F** and m/z 155 $[BTMSA–Me]^+$ for **1D–1E**. Although the molecular ions were not observed for the less volatile compounds the fragment ions do not originate from the ionization of products of the thermolysis. Should it be so, the least volatile **1F** would afford m/z 316 (M^+) of **2F** and the MS spectrum of 1,2-bis(trimethylsilyl)ethene (vide infra).

3.1. Crystal structure of 1E

It follows from the spectroscopic data that compounds **1A–1E** have the same structure as **1F** whose X-ray structure is known [9,10]. The molecular structure of **1E** is, however, of interest as it may throw light on the reason for different catalytic activity of **1F** and **1E** towards terminal acetylenes [25]. The molecular structure of **1E** (Figure 1) is, in contrast to that of **1F**, symmetrical with respect to a twofold axis which contains the Ti atom and bisects the acetylenic C–C bond. Since the accuracy of X-ray structure determination for both **1E** and **1F** is comparable the molecular parameters of both the compounds listed in Table 3 can provide a

Table 6
NMR (δ ppm) and IR (cm^{-1}) data on the BTMSA ligand in **1A–1F**

Cpd	^{1}H(Me)	^{13}C(Me)	^{13}C(C≡C)	^{29}Si	ν(C≡C) [a]
1A	−0.333 s	0.59 q [b]	244.77 s [b]	−14.41 [b]	1662
1B	−0.270 s	1.18 q	245.28 s	−15.41	1659
1C	−0.228 s	1.54 q	245.54 s	−16.06	1657
1D	−0.118 s	2.31 q	246.35 s	−16.36	1627
1E	−0.049 s	3.46 q	248.35 s	−17.18	1609
1F	0.016 s	4.23 q	248.51 s	−17.29	1598

[a] Average value of wavenumbers of absorption bands in the region of ν(C≡C) vibration of coordinated BTMSA.
[b] Chemical shifts for non-coordinated BTMSA (C_6D_6, 23°C): ^{13}C(Me) δ 0.23 q, ^{13}C(C≡C) δ 113.84 s, ^{29}Si δ −19.3 ppm [24].

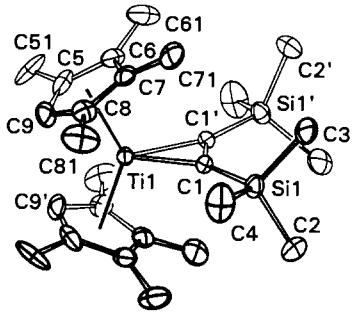

Fig. 1. ORTEP diagram of **1E** with 50% probability thermal ellipsoids and atom numbering scheme.

good basis for evaluation of steric effects. The most remarkable difference is observed for the dihedral angle ϕ contained by the least-squares planes of the cyclopentadienyl rings in **1F** and **1E**. This follows from a large steric hindrance between the Me substituents of the C_5Me_5 ligands in positions where the ligands approach each other in a staggered conformation. In **1E**, the C_5HMe_4 ligands are in staggered conformation and the positions of close contacts are occupied by hydrogen atoms. Thus, the steric hindrance between the C_5HMe_4 ligands is strongly diminished and as a result, angle ϕ in **1E** is by 8.9° larger than in **1F**. The value of ϕ 50.0° and the CE–Ti–CE angle 134.9° imply that the CE–Ti connection in **1E** is not perpendicular to the ring plane and that the Ti atom is shifted towards the apex of the angle ϕ. A similar shift of the Ti atom was found also in $(C_5HMe_4)_2TiCl$, $(C_5HMe_4)_2TiI$, and $(C_5HMe_4)_2TiCl_2$ [26]. The CE–Ti–CE angles in the above halides reached the values 139.1°, 139.3° and 133.4°, respectively, and it is remarkable that the value of CE–Ti–CE angle in **1E** (134.9°) is close to that for $(C_5HMe_4)_2TiCl_2$. The CE–Ti–CE angle seems to be generally smaller in titanocene complexes with the pseudotetrahedral symmetry [27] than in trigonally coordinated monohalides [26]. The effect is probably aided by the mutual repulsion between the C_5HMe_4 ligands at the open side of the $(C_5HMe_4)_2Ti$ moiety and the chlorine atoms or BTMSA.

The coordinated BTMSA ligand has the C–C bond length close to that of a double bond and the substantial contribution of sp^2 hybridization at these carbon atoms is reflected in a large bending of $SiMe_3$ groups from the linear configuration farther away from the titanium atom. The Ti–C_{ac} bonds are discernibly (by 0.02 Å) and the C_{ac}–C_{ac} and Si–C_{ac} bonds marginally longer (by less than 0.01 Å) in **1F** compared to **1E** (cf. Table 3). The prolonged Ti–C_{ac} and Si–C_{ac} bonds in **1F** can be accounted for by the presence of steric hindrance between the open side of the $(C_5Me_5)_2Ti$ moiety and the BTMSA ligand. On the other hand, the difference in the Ti–$C(C_5Me_5)_{av}$ and Ti–$C(C_5HMe_4)$ distances (in **1F** by 0.02 Å longer than in **1E**) was found to be the same as between $(C_5Me_5)_2TiCl_2$ [28] and $(C_5HMe_4)_2TiCl_2$ [26]. It means that if there is any hindrance between the BTMSA ligand and the C_5Me_5

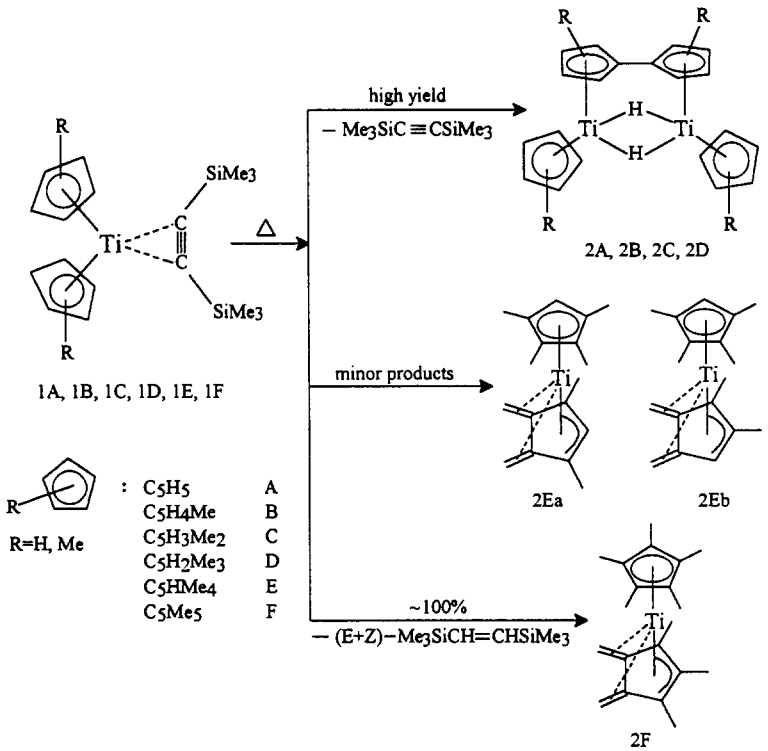

Scheme 1.

Table 7
Infrared and electronic absorption spectra of **2A–2D** [a]

Compound	ν(Ti–H–Ti) (cm^{-1})	UV-Vis (nm)		
2A	1227	432	780 [b]	828
2B	1213	432	770 [b]	828
2C	1206, 1180	434	770 [b]	840
2D	1166, 1134	434	780 [b]	862

[a] In hexane solutions.
[b] Shoulder.

ligands it causes a slight repulsion of the BTMSA ligand but does not affect the $(C_5Me_5)_2Ti$ skeleton.

3.2. Thermal decomposition of 1A–1F

All the complexes decompose at temperatures 100–200°C depending on the number of Me groups in the $C_5H_{5-n}Me_n$ ($n = 0–5$) ligands. The decomposition temperature increases from 100°C for **1A** to 200°C for **1E** but **1F** decomposes at only 130°C. Compounds **1A–1E** release one equivalent of BTMSA whereas **1F** liberates a mixture of *cis*- and *trans*-1,2-bis(trimethylsilyl)ethene (see Scheme 1). Compounds **1A–1D** decompose in a uniform way to give 'dimeric titanocene', $(\mu\text{-}\eta^5\text{:}\eta^5\text{-}C_{10}H_8)[(\eta^5\text{-}C_5H_5)Ti(\mu\text{-}H)]_2$ (**2A**) and its methylated analogues (**2B–2D**) in high yields. These compounds are easily identified by electronic absorption spectra which are characterized by a very intense band above 800 nm accompanied by a shoulder at its shorter wavelength side. This band is shifted to higher wavelengths upon introduction of Me groups into the cyclopentadienyl ligands of their parent compounds **1A–1D** (see Table 7). The nature of this transition as well as the electronic structure of the complexes is not known. The NMR spectra exert broad lines at room temperature which are difficult to be assigned. The ^1H NMR spectrum of **2A** was previously measured in the temperature range −60°C–25°C and showed the narrowing of signals with decreasing temperature [29]. This behaviour was attributed to an admixture of a thermally populated triplet state to an essentially ground singlet state of **2A**. The present series of methylated compounds affords a chance for assignment of NMR spectra of dimeric titanocenes provided a detail study at various temperatures is carried out.

Infrared spectra of **2A–2D** are dominated by an intense absorption band near 1200 cm^{-1} (Table 7) which has been for **2A** assigned to the valence vibration of bridging Ti–H–Ti bonds [19]. This broad absorption band is split in **2C** and **2D** and relative intensities of the two bands are interchanged when measured in toluene solution and in KBr pellet. This splitting may arise from an asymmetrical arrangement of di- and tri-methylated cyclopentadienyl rings in a manner similar to that found in the solid state for **2D** (vide infra). The wavenumbers of this band or the average of the two bands, respectively, are decreasing with increasing number of Me substituents. Thus indicated weakening of the Ti–H–Ti bonds is in accord with a longer Ti–Ti distance in **2D** (3.096(2) Å) compared to that in **2A** (2.989(1) Å) [30] (vide infra). The mass spectra of **2A–2D** are characterized by an extensive loss of hydrogen from ionized molecules (cf. [19]). The molecular ion intensity is increasing from **2A** (23%) to **2C** (59%) but it falls down to 18% for **2D**. The reference intensity peaks (100%) were $(M-4H)^+$ for **2A**, $(M-6H)^+$ for **2B** and **2C** and $(M-8H)^+$ for **2D**. Clusters of peaks differing by mass units were obtained for fragment ions $(M-Me)^+$ (not observed for **2A**), $(M-C_5H_{5-n}Me_n$, $n = 0–3)^+$, $(M-(C_5H_{5-n}Me_n)_2TiH)^+$, and $((C_5H_{5-n}Me_n)Ti)^+$.

The fulvalene complexes **2A–2D** were apparently formed through the generation of intermediate titanocene and methyl-substituted titanocenes. BTMSA was recovered, according to GC analysis quantitatively and hence, titanocene compounds dimerized with intramolecular hydrogen transfer to form the fulvalene ligand and $Ti(\mu\text{-}H)_2Ti$ bridge. This method of preparation of **2A–2D** yields cleaner products than the method based on the reduction of $(C_5H_{5-n}Me_n)_2TiCl_2$ by $LiAlH_4$ in high-boiling aromatic solvents [13] where the mixed chlorohydrido complexes can be present as impurities.

Analogous formation of the octamethylfulvalene complex from **1E** does not occur probably because of the steric hindrance of Me groups in inner positions of the fulvalene ligand. A mixture of brown products was obtained from the thermolysis of **1E**, however, no individual compound has been isolated by fractional crystallization. The sublimation of the solid products afforded a low yield of a mixture of asymmetric $(\eta^3\text{:}\eta^4$-1,2-dimethyl-4,5-dimethylenecyclopentenyl)$(\eta^5$-tetramethylcyclopentadienyl)titanium (**2Eb**) and symmetric $(\eta^3\text{:}\eta^4$-1,3-dimethyl-4,5-dimethylenecyclopentenyl)$(\eta^5$-tetramethylcyclopentadienyl)titanium (**2Ea**) in the ratio ca. 8:1. They were previously obtained in a similar low yield and mutual abundance by sublimation of the solid product obtained from the reduction of $(C_5HMe_4)_2TiCl_2$ by $LiAlH_4$ in toluene [20].

Compound **1F** afforded previously described blue 'allyl-diene titanium complex', $(\eta^3\text{:}\eta^4$-1,2,3-trimethyl-4,5-dimethylenecyclopentenyl)(pentamethylcyclopentadienyl)titanium (**2F**) [21] in quantitative yield. In this case volatiles contained a mixture of *cis*- and *trans*-1,2-bis(trimethylsilyl)ethene and no BTMSA. This implies that an intermediate titanocene species was liberated with a simultaneous hydrogen transfer to BTMSA. The thermolysis of **1F** is the superior method of synthesis of **2F** as the previously reported methods based on the thermolysis of the $(C_5Me_5)_2TiR$ or $(C_5Me_5)_2TiH$ compounds [21] or on the sublimation of the residue ob-

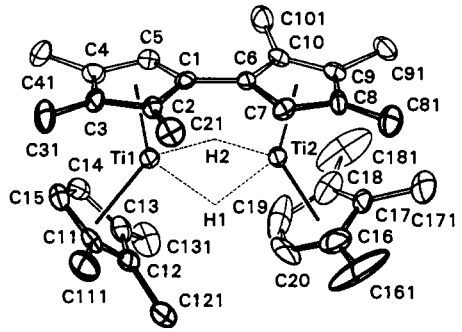

Fig. 2. ORTEP diagram of **2D** with 50% probability thermal ellipsoids and atom numbering scheme. Bridging hydrogen atoms were not located and are drawn schematically.

tained from the $(C_5Me_5)_2TiCl_2$/$LiAlH_4$/toluene system [20] afforded max. 30% yield.

3.3. Crystal structure of 2D

The X-ray crystal structure of **2D** corroborates conclusions based on IR and UV-Vis spectra that it is an analogue of dimeric titanocene $(\mu\text{-}\eta^5\text{:}\eta^5\text{-}C_{10}H_8)[(\eta^5\text{-}C_5H_5)Ti(\mu\text{-}H)]_2$, **2A**, although it has been determined with a low accuracy and positions of bridging hydrogen atoms were not identified. The ORTEP diagram of **2D** (Figure 2) thus shows these hydrogen atoms placed close to positions known for **2A** whose crystal structure is known [30]. The hexamethylfulvalene ligand contains ring protons in inner positions on alternate sides with respect to the least-squares plane defined by the Ti(1), Ti(2), C(1) and C(6) atoms. The ligand is bent with the rings inclined to the titanium atoms. The dihedral angle between the fulvalene ring planes $\omega = 10.5°$ is smaller than in **2A**, where $\omega = 17.7°$. This is in accordance with a slightly longer Ti–Ti distance 3.096(2) Å compared to 2.989(1) Å in **2A** and Ti–C_{fulv} distances 2.29–2.48 Å (for both CE(1) and CE(2) rings) compared to 2.30–2.39 Å in **2A**. The shortest Ti–C_{fulv} distances belong to the inner carbon atoms. The titanium atoms are bound virtually equally to the fulvalene rings with the Ti–CE(1) and Ti–CE(2) distances 2.063(10) Å and 2.064(10) Å and with distances between the Ti atoms and the ring planes 2.050(10) Å and 2.052(10) Å, respectively. On the other hand, the cyclopentadienyl ligands are oriented asymmetrically. The CE(3) ring methyl groups are directed towards bridging hydrogen atoms whereas the CE(4) ring methyls point to the fulvalene ligand. This conformation induces a large difference in dihedral angles between the least-squares planes of the CE(1) and CE(3) rings 47.0° and the CE(2) and CE(4) rings 31.9° and a smaller value of the CE(1)–Ti(1)–CE(3) angle 133.1(1)° compared to that of CE(2)–Ti(2)–CE(4) 138.4(1)°. The bridging hydrogen atoms are probably inequivalent as the CE(3) ring is placed asymmetrically with respect to the least-squares plane defined by the Ti atoms and C(1) and C(6) atoms. This can bring about the observed splitting of the IR absorption band of the ν(Ti–H–Ti) vibration (vide supra).

4. Supplementary material available

Listings of atomic coordinates and isotropic thermal parameters, and all bond distances and angles are available from the Fachinformationszentrum Karlsruhe, Gesellschaft für wissenschaftlich-technische Information mbH, D-76012 Karlsruhe by quoting the deposition number CSD-58523, and these together with anisotropic thermal parameters, least-squares planes, dihedral angles, observed and calculated structure factors and views of unit cell may be obtained from the authors.

Acknowledgements

Authors thank Doc. Dr. Jan Schraml for recording ^{29}Si NMR spectra. This investigation was supported by the Grant Agency of Academy of Sciences of the Czech Republic, grant no. 440403, by the Grant Agency of the Czech Republic, grant no. 203/93/0143, and by the Fonds der Chemischen Industrie.

References

[1] D.J. Sikora, J.W. Macomber and M.D. Rausch, *Adv. Organomet. Chem., 25* (1986) 317.
[2] M.D. Fryzuk, T.S. Haddad and D.J. Berg, *Coord. Chem. Rev. 99* (1990) 137.
[3] (a) G. Fachinetti and C. Floriani, *J. Chem. Soc., Chem. Commun.*, (1974) 66; (b) G. Fachinetti, C. Floriani, F. Marchetti and M.J. Mellini, *J. Chem. Soc., Dalton Trans.*, (1978) 1398.
[4] (a) B. Demerseman and P.H. Dixneuf, *J. Chem. Soc., Chem. Commun.* (1981) 665; (b) B. Demerseman, G. Mahe and P.H. Dixneuf, *J. Chem. Soc., Chem. Commun.*, (1984) 1394; (c) B.Demerseman, P. Le Coupanes and P.H. Dixneuf, *J. Organomet. Chem., 287* (1985) C35.
[5] B.H. Edwards, R.D. Rogers, D.J. Sikora, J.L. Atwood and M.D. Rausch, *J. Am. Chem. Soc., 105* (1983) 416.
[6] S.A. Cohen and J.E. Bercaw, *Organometallics, 4* (1985) 1006.
[7] V.B. Shur, V.V. Burlakov and M.E. Vol'pin, *J. Organomet. Chem., 347* (1988) 77.
[8] V.V. Burlakov, U. Rosenthal, P.V. Petrovskii, V.B. Shur and M.E. Vol'pin, *Metalloorg. Khim., 1* (1988) 953.
[9] V.V. Burlakov, U. Rosenthal, R. Beckhaus, S.V. Polyakov, Yu.T. Struchkov, G. Oehme, V.B. Shur and M.E. Vol'pin, *Metalloorg. Khim., 3* (1990) 476.
[10] V.V. Burlakov, A.V. Polyakov, A.I. Yanovsky, Yu.T. Struchkov, V.B. Shur, M.E. Vol'pin, U. Rosenthal and H. Görls, *J. Organomet. Chem., 476* (1994) 197.
[11] U. Rosenthal, H. Görls, V.V. Burlakov, V.B. Shur and M.E. Vol'pin, *J. Organomet. Chem., 426* (1992) C53.
[12] U. Rosenthal, G. Oehme, V.V. Burlakov, P.V. Petrovskii, V.B. Shur and M.E. Vol'pin, *J. Organomet. Chem., 391* (1990) 119.
[13] H. Antropiusová, A. Dosedlová, V. Hanuš and K. Mach, *Transition Met. Chem., 6* (1981) 90.

[14] K.C. Ott, E.J.M. DeBoer and R.H. Grubbs, *Organometallics, 3* (1984) 223.
[15] V. Varga, K. Mach, G. Schmid and U. Thewalt, *J. Organomet. Chem., 475* (1994) 127.
[16] K. Mach, V. Varga, H. Antropiusová and J. Poláček, *J. Organomet. Chem., 333* (1987) 205.
[17] J. Schraml, *Coll. Czech. Chem. Commun. 48* (1983) 3402.
[18] V. Varga, K. Mach, G. Schmid and U. Thewalt, *J. Organomet. Chem., 454* (1993) C1.
[19] H.H. Brintzinger and J.E. Bercaw, *J. Am. Chem. Soc., 92* (1970) 6182.
[20] K. Mach, V. Varga, V. Hanuš and P. Sedmera, *J. Organomet. Chem., 415* (1991) 87.
[21] J.W. Pattiasina, C.E. Hissink, J.L. de Boer, A. Meetsma, J.L. Teuben and A.L. Spek, *J. Am. Chem. Soc., 107* (1985) 7758.
[22] R. Brüggemann, T. Debaerdemaeker, B. Müller, G. Schmid and U. Thewalt, *ULM-Programmsystem*, 1. Jahrestagung der Deutschen Gesellschaft für Kristallografie, Mainz, June 9–12, 1992, Abstracts, p. 33, which includes the SHELX-76 Program for Crystal Structure Determination by G.M. Sheldrick, University of Cambridge, Cambridge, England, 1976.
[23] P.T. Witte, V. Varga and K. Mach, II. Regional Seminar of PhD Students in Organometallic Chemistry, Prague, December 1994; Abstracts, p. 52.
[24] M.I.Al-Hassan, I.M. Al-Najjar and I.M. Al-Oraify, *Magn. Resonance Chem., 27* (1989) 1112.
[25] V. Varga, L. Petrusová, J. Čejka and K. Mach, *J. Organomet. Chem.*, in press.
[26] S.I. Troyanov, V.B. Rybakov, U. Thewalt, V. Varga and K. Mach, *J. Organomet. Chem., 447* (1993) 221–225.
[27] D. Cozak and M. Melnik, *Coord. Chem. Rev., 74* (1986) 53.
[28] T.C. McKenzie, R.D. Sanner and J.E. Bercaw, *J. Organomet. Chem., 102* (1975) 457.
[29] D.A. Lemenovskii, I.F. Urazowski, Yu.K. Grishin and V.A. Roznyatovsky, *J. Organomet. Chem., 290* (1985) 301.
[30] S.I. Troyanov, H. Antropiusová and K. Mach, *J. Organomet. Chem., 427* (1992) 49.